Journal of Advanced Pharmaceutical Sciences

Journal homepage: https://japs.journals.ekb.eg/

Research article

Kiwi-derived N-doped green carbon dots: Antioxidant and anti-inflammatory potential for hyperglycemia control

Riham M. El-Moslemany, Amal H. El-Kamel, Mai O. Soliman, Asmaa A. Ashour*

Department of Pharmaceutics, Faculty of Pharmacy, Alexandria University, Alexandria, Egypt

***Corresponding author:** Department of Pharmaceutics, Faculty of Pharmacy, Alexandria University, 1 Khartoum Square, Azarita, Messalla Post Office, Postal code: 21521, Alexandria, Egypt.

Tel: 002 01009298839, Fax: 00203- 4873273

E-mail: Asmaa.ashour@alexu.edu.eg

Abstract:

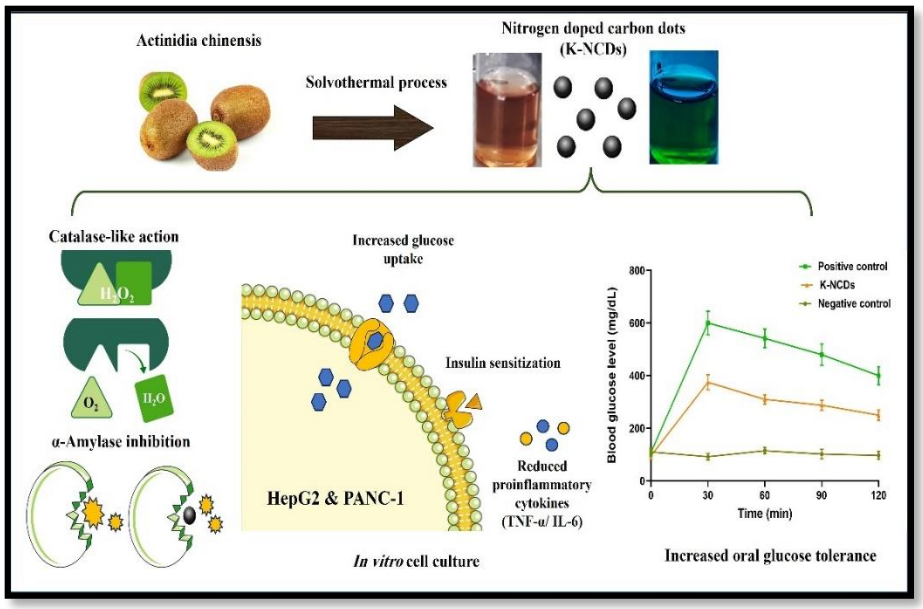

Diabetes mellitus is a major global health problem characterized by chronic hyperglycemia, which can lead to serious complications if left untreated. In the recent years, the development of novel diagnostic and therapeutic tools for diabetes has become increasingly important. Among emerging approaches, the green synthesis of nanomaterials has drawn significant interest due to its eco-friendly nature. This study investigates the use of kiwifruit as a sustainable carbon precursor with triethanolamine as a nitrogen dopant for the phyto-mediated production of carbon dots (K-NCDs) utilizing a simple solvothermal technique. The produced K-NCDs were thoroughly characterized using UV–Visible spectroscopy, fluorescence spectrophotometry, FT-IR, X-ray diffraction (XRD), transmission electron microscopy, and others. The K-NCDs had an average size of 9.2±3 nm, a ζ-potential of -26.1±1.85 mV, and a quasi-spherical morphology. They exhibited an intense green emission under the excitation of 275 nm, with FT-IR analysis proving nitrogen doping and XRD verifying their amorphous structure. Biological activity evaluation demonstrated potent antioxidant and hypoglycemic effects.

Received: 13 May 2025 Accepted: 28 May 2025 Published: 30 May 2025

ISSN: 3009-7061 **DOI: 10.21608/japs.2025.384682.1051**

At a concentration of 5 mg/mL, K-NCDs achieved 99.6 % 2,2-diphenyl-1-picrylhydrazyl inhibition and a dose-dependent catalase-like activity. They also inhibited α-amylase, a key target for managing type 2 diabetes, by 79.7±2.66%. *In vitro* insulin-sensitizing assays on insulin-resistant HepG2 and PANC-1 cells revealed enhanced glucose at concentrations of 25-100 μg/mL. Moreover, oral hypoglycemic efficacy was confirmed in a streptozocin-induced diabetic rat model following a single 400 mg/kg oral dose. The study findings support the use of K-NCDs as a promising, eco-friendly therapeutic option for hyperglycemia.

Keywords: Kiwi, Solvothermal, Nitrogen-Doped, Antioxidant, Glucose Uptake

1. Introduction

The International Diabetes Federation (IDF) Diabetes Atlas estimates that ~ 589 million adults worldwide between the ages of 20 and 79 presently have diabetes, and that number is expected to increase to 853 million by 2050 [(1)]. Hyperglycemia is a hallmark feature of diabetes and represents a significant health concern, particularly among individuals dependent on insulin or other glucose-lowering therapies. Despite advancements in the management of diabetes, persistent hyperglycemia continues to pose a major clinical challenge. It is closely associated with the development of serious complications, including cognitive impairment, cardiovascular events, and, in extreme cases, death [(2)]. The development of innovative strategies to prevent or mitigate hyperglycemic episodes while maintaining optimal glycemic control is therefore a pressing need in diabetes care.

Nanotechnology has become a promising area of biomedical research in recent years, providing innovative approaches to therapeutic interventions, medication delivery, and diagnostics [(3)]. Carbon dots (CDs) represent a class of fluorescent carbon-based nanomaterials that have attracted a lot of interest because of their special qualities, which include low toxicity, biocompatibility, and adjustable bioactivity [(4)].

Natural product-derived carbon dots (NPCDs), which are synthesized from sustainable and renewable sources such as fruits, vegetables, and herbs, have shown immense potential in biomedical applications due to their inherent bioactive properties and sustainability [(5)]. For instance, NPCDs are produced from a variety of natural sources, including coffee [(6)], pomegranate [(7)], turmeric [(8)], orange, and garlic, among others [(9)]. Compared to conventional CDs, NPCDs may contain bioactive ingredients extracted from their precursors, such as phenolic compounds, flavonoids, or polysaccharides. These constituents grant specific biological activities and medicinal properties to NPCDs [(10)].

Despite the expansion of recent research on the intrinsic bioactivities of CDs, it revolves around basic facets, e.g., fluorescent properties, and their application in clinical practice as hypoglycemic agents is not investigated thoroughly.

The hypoglycemic effects of NPCDs are thought to be mediated through multiple mechanisms. These include enhancing insulin sensitivity, promoting glucose uptake in peripheral tissues, inhibiting hepatic gluconeogenesis, and modulating gut microbiota [(10)]. It is important to highlight that carbohydrate degradation rate during digestion has been connected with the regulation of postprandial insulin and blood glucose levels. Sucrase and maltase are two essential intestinal enzymes involved in carbohydrate breakdown and glycoprotein biosynthesis. A strategy holding great promise as hypoglycemic agents is through

ISSN: 3009-7061 **DOI: 10.21608/japs.2025.384682.1051**

developing approaches targeting inhibition of these enzymes or enhancing carbohydrate degradation rate [11]. In this context, Lu *et al*. developed CDs from the traditional Chinese medicinal plant *Fructus Crataegi.* They revealed their ability to potentially function as inhibitors of disaccharidase, thus reducing postprandial blood glucose levels effectively in humans and inhibiting *in vitro* maltase and sucrase catalytic activity [12].

Similarly, Sun *et al*. used pyrolysis to create Jiaosanxian-derived CDs (JSX-CDs), with an average diameter of 4.4 – 6.4 nm. The great solubility and biological activity of JSX-CDs are attributed to their numerous surface groups. They found that these CDs considerably lowered the blood glucose levels of hyperglycemic mice. Moreover, they showed that JSX-CDs regulated blood sugar levels while fasting without producing hypoglycemia symptoms, indicating their capacity as an unprecedented class of hypoglycemic drugs [13].

Kiwifruit (*Actinidia chinensis*), a nutrient-rich fruit known for its high levels of vitamin C, polyphenols, and dietary fiber, has been broadly studied for its anti-inflammatory, antioxidant, and antidiabetic effects [5]. It has been reported that kiwifruit exhibited other biological activities such as anti-hypertensive, hepatoprotective, anti-asthmatic, antiviral, antifungal, anti-nociceptive, anti-microbial, anti-constipation, anti-platelet, and anti-thrombin activity [14]. Catechin, rutin, and epicatechin are the main flavonoids found in kiwifruit [15]. The anti-diabetic, anti-inflammatory, and antioxidant properties of a mixture of the three kiwi main flavonoids were verified in mice [16]. These properties make kiwi-derived CDs a promising candidate for addressing the hyperglycemia effect.

Kiwi-derived carbon dots (K-CDs) are particularly intriguing due to their potential to combine the inherent bioactivity of kiwi with the unique properties of carbon-based nanomaterials. It is worth mentioning that green fluorescent nitrogen-doped carbon dots (NCDs) using kiwifruit extract as a carbon precursor exhibited low cytotoxicity and hence high biocompatibility on MCF-7 and L-929 cells [17]. Kiwifruit peel-CDs synthesized by Atchudan *et al*. were shown to be nontoxic to both normal and cancerous cells, which is crucial for the sustainable development of agents for cellular imaging [18].

Triterpenoids and flavonoids present in kiwi fruit have been reported to significantly inhibit the *in vitro* activity of α-glucosidase and α-amylase, possibly delaying starch digestion [19]. Additionally, it has been demonstrated that kiwifruit is a good source of antioxidants, which help reduce oxidative stress as one of the major factors for diabetes development. By lowering oxidative stress, kiwifruit preserves pancreatic β-cells and improves insulin production. Kiwifruit also has anti-inflammatory properties that help reduce levels of pro-inflammatory cytokines, including IL-1β and TNF-α. These pro-inflammatory cytokines are involved in the autoimmune process in type 1 diabetes. Therefore, the anti-inflammatory potential of kiwifruit supports insulin synthesis and β-cell function. In diabetic rats, kiwifruit peel extract improves markers for inflammation and oxidative stress, including reduced glutathione (GSH) and nitric oxide (NO) [20]. Overall, kiwifruit's hypoglycemic effect is ascribed to its anti-inflammatory, antioxidant, and enzyme-inhibitory properties, which make it a promising treatment option for diabetes [20].

This research seeks to contribute to the development of innovative therapeutic strategies for hyperglycemia. Within this framework, our study aims to investigate the hypoglycemic effects of nitrogen-doped kiwi-derived carbon dots (K-NCDs), leveraging their dual advantages as a natural product and a nanomaterial, focusing on their

ISSN: 3009-7061 **DOI: 10.21608/japs.2025.384682.1051**

mechanisms of action and therapeutic potential. We use both *in vitro* and *in vivo* models to elucidate the pathways through which K-NCDs modulate glucose metabolism and evaluate their efficacy in preventing hypoglycemic episodes. Furthermore, this research explores the safety of K-NCDs, ensuring their suitability for clinical applications. The findings could pave the way for the application of K-NCDs as a novel, natural, and safe intervention for individuals at risk of hyperglycemia, addressing a critical gap in current diabetes care.

2. Materials and methods

2.1. Materials

Kiwifruits were purchased from the local market in Alexandria, Egypt. Triethanolamine (TEA) and ethanol were from Fischer Scientific (Loughborough, UK). Streptozotocin was purchased from Sigma-Aldrich (St. Louis, USA). A commercial Glucose kit was obtained from BioMED Pharmaceutical Industries (Cairo, Egypt). All other chemicals and reagents were of analytical grade.

2.2. Synthesis of nitrogen-doped carbon dots (K-NCDs)

K-NCDs were prepared using kiwifruit juice and TEA as carbon and nitrogen precursors, respectively (**Fig. 1**). Briefly, 30 mL of the juice was mixed with absolute ethanol (20 mL), followed by adding triethanolamine (1 mL) with thorough mixing. Transfer to a Teflon lined autoclave followed by heating for 3 h at 200°C was done. The mixture was allowed to cool to room temperature, then centrifuged for 15 min at 15,000 rpm to remove any gross particles. Finally, the dispersion was filtered by a membrane filter (0.22 µm) for further purification.

2.3. *In vitro* characterization of K-NCDs

2.3.1.X-ray diffraction (XRD)

Dried K-NCDs crystallinity was assessed using XRD (XRD-7000 X-Ray diffractometer, Bruker D2-Phaser; Madison, WI, USA) by a step scan model of 30 kV and 30 mA. The diffraction angle (2θ) scanning region was set at a 0.02º step size from 0 to 100°.

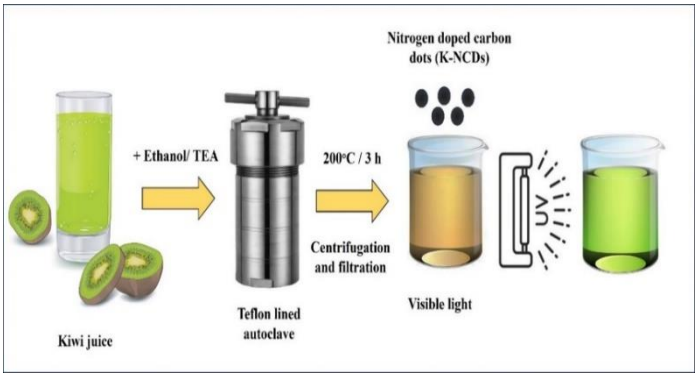

Fig. 1: Schematic representation of K-NCDs preparation from kiwifruit juice.

2.3.2. Fourier transform infrared spectrum (FT-IR)

The FTIR spectrum of K-NCDs was obtained using an FT-IR spectrometer (PerkinElmer Inc., USA) by scanning in the range 4000–700 cm^{-1}. Prior to analysis, 1 mL of K-NCDs was allowed to dry in an oven at 70°C. The dried sample was mixed with KBr and compressed into a disk.

2.3.3. Morphological examination and particle size measurement

Transmission electron microscopy (TEM) (model JEM-100CX, JEOL, Japan) was used for morphological assessment of K-NCDs as well as for the determination of the average particle size. The sample was placed on a carbon-coated copper grid, air-dried then examined. Shots were taken at 50 K magnification. Particle size (PS) was determined using Image-J analysis software (Fiji 1.52p; National Institutes of Health, Bethesda, MD, USA) based on 100 measurements from different fields.

The surface morphology of K-NCDs was further appraised using scanning electron microscopy (SM-IT200; JEOL, Tokyo, Japan). Before examination, the sample was placed on a metal stub, air-dried then gold

ISSN: 3009-7061 **DOI: 10.21608/japs.2025.384682.1051**

sputter-coated.

2.3.4. ξ-potential measurement

ζ-potential of K-NCDs was measured using Malvern Zetasizer (Nano-ZS Series DTS 1060, Malvern Instruments, UK). This was done at 25°C at a fixed angle of 173◦ following adequate dilution of the sample (n=3).

2.3.5. Optical properties

The optical properties of K-NCDs were assessed *by* studying their UV-vis absorbance and fluorescence spectra. The UV-vis spectrum was obtained (Cary 60 UV–Visible spectrophotometer, Agilent, USA) in the wavelength range 200-400 nm, whereas fluorescence spectroscopy measurements were made using Cary Eclipse Fluorescence Spectrophotometer (Agilent, USA) at different excitation wavelengths (240-280 nm).

2.3.6. Relative quantum yield

The quantum yield (QY) of K-NCDs was determined relative to fluorescein isothiocyanate (FITC, QY = 92 %). For relative QY assessment, five dilutions of each of FITC and K-NCDs with absorbance less than 0.05 were prepared. The fluorescence intensity of the samples was measured at the excitation wavelength of K-NCDs. Then, the slope of the linear plots of absorbance vs integrated fluorescence intensity was determined, and the QY was calculated using equation (1):

$$\varphi = \varphi' \frac{m}{m'} \left(\frac{\eta}{\eta'}\right)^2 \quad (1)$$

Where, φ', m', η' are the QY, slope, and solvent refractive index of FITC solution, respectively, while φ, m, and η are the QY, slope, and solvent refractive index of K-NCDs, respectively.

2.3.7. Antioxidant 2,2-Diphenyl-1-picrylhydrazyl assay (DPPH)

The free radical scavenging activity of K-NCDs was tested using the DPPH assay. Different concentrations of K-NCDs (1.25, 2.5, and 5 mg/mL) were examined for their antioxidant capacity. In a test tube, DPPH (50 µM methanolic solution) and samples were mixed in a ratio of 1:1 by volume. The tubes were vigorously shaken and then kept for 30 min in the dark at room temperature. Absorbance measurement was done at 517 nm. The percentage of antioxidant activity was then calculated by equation (2):

$$\%\ Antioxidant\ activity = \left(\frac{absorbance\ of\ control - absorbance\ of\ sample}{absorbance\ of\ control}\right) x\ 100 \quad (2)$$

Where the absorbance of the control and sample are the absorbances of DPPH solution (not containing K-NCDs) and sample solution (containing K-NCDs), respectively.

2.3.8. Catalase-like activity assay

The antioxidant catalase-like activity of K-NCDs was measured using the RayBio® colorimetric assay kit (#MA-CAT) according to the manufacturer's instructions. Briefly, 20 µL of the K-NCDs samples (1.25, 2.5, and 5 mg/mL) were placed in a 96-well plate, then 30 µL of 1 mM H_2O_2 was added to each well and thoroughly mixed, followed by incubation at room temperature for 1 min. Catalase quencher (50 µL) was added and mixed for 5 min to stop the reaction. After 15 min of stopping the reaction, chromogenic working solution (150 µL) was added to each well and incubated for 15 min at room temperature with gentle mixing. Lastly, using a plate reader, the UV-Visible absorbance was measured at 520 nm, and enzyme-like activity was extrapolated from the standard curve.

2.3.9. Glucose uptake by yeast cells

The test was performed as previously described by Rehman *et al*. [21]. Baker's yeast dissolved in distilled water (1% w/v) was washed by repeated centrifugation. A 10% suspension was then prepared in distilled water. Increasing concentrations of K-NCDs (0.5–5 mg/mL) were mixed with 25 mM glucose solution (1 mL), followed by incubation at 37°C for 10 min. Reaction initiation was done by the addition of yeast suspension (100 µL), followed by vortexing

ISSN: 3009-7061 **DOI: 10.21608/japs.2025.384682.1051**

and incubation for 60 min at 37°C. Thereafter, centrifugation (2,500 × g, 5 min) was done, and glucose concentration in the supernatant was measured at 540 nm. The percentage increase in glucose uptake by yeast cells was calculated using equation (3):

$$\%\ Increase\ in\ glucose\ uptake = \left(\frac{absorbance\ of\ control - absorbance\ of\ sample}{absorbance\ of\ control}\right) x\ 100 \quad (3)$$

Where control is the solution that contains all the components, excluding K-NCDs.

2.3.10. α-amylase inhibition assay

The ability of K-NCDs to inhibit α-amylase was evaluated using the 3,5-dinitrosalycilic acid (DNSA) method [22]. Briefly, α-amylase was diluted using 0.02 M PBS/ 0.006 M NaCl (pH 6.9) to 2 units/mL. K-NCDs (1.25, 2.5, and 5 mg) were mixed with 0.2 mL of α-amylase and vortexed mixed then incubated at 30°C for 10 min. This was followed by mixing with 0.2 mL maize starch solution (1% w/v) in deionized water and incubation at room temperature for 3 min. Reaction termination was done using 200 µL of 3,5-dinitrosalycilic acid (DNSA) stop solution (sodium potassium tartrate tetrahydrate solution in 2 M NaOH and 96 mM of DNSA solution in the ratio 2:5) and heating in 85-90°C water bath for 10 min. Reaction mixtures were allowed to cool to room temperature, then filtered using a syringe filter (0.45 µm). Filtrates were diluted using deionized water (6-fold) and spectrophotometrically analyzed at 540 nm. A control sample for background correction was prepared similarly by sample replacement with 0.2 mL PBS, representing 100% enzyme activity. α-amylase inhibitory activity was calculated using equation (4):

$$\%\ \alpha - \text{amylase}\ inhibition = \left(\frac{absorbance\ of\ control - absorbance\ of\ sample}{absorbance\ of\ control}\right) x\ 100 \quad (4)$$

2.4. *In vitro* cell culture studies

2.4.1. Cell culture

HepG2 and PANC-1 cells were obtained from the American Type Culture Collection (ATCC, Manassas, VA, USA). Cells were cultured under 5% CO_2 at 37 °C. The culture medium comprised Dulbecco's Modified Eagle's Medium (DMEM, Biowest, France) supplemented with fetal bovine serum (10% FBS, Biowest, France), 1% streptomycin, and 100 U/mL penicillin (Invitrogen, Grand Island, NY, USA). The studies were carried out at the Cell Culture Lab, Department of Pharmaceutics, Faculty of Pharmacy, Alexandria University.

2.4.2. Cell-viability assay

Tetrazolium salt, 3-(4,5-dimethylthiazol-2-yl)-2,5-diphenyltetrazolium bromide (MTT) was used to investigate K-NCDs effect on HepG2 and PANC-1 cell viability. Cells were seeded at a seeding density of 1×10^4 cells/well in a 96-well plate, followed by 24 h incubation. Thereafter, medium replacement with one containing increasing concentrations of K-NCDs (2-100 µg/mL), then incubation for 48 h at 37 ºC and 5% CO_2 was done. MTT (0.5 mg/mL final concentration) dissolved in PBS was then added to the wells, and the plate was incubated for 4 h at 37 °C. For each well, media aspiration followed by formazan crystals dissolution in 100 µL dimethyl sulfoxide (DMSO) was carried out. Absorbance was measured by an ELISA well-plate reader (BioTek, USA) at 570 nm. Percentage viability calculation relative to control cells was then done (n=3).

2.4.3. Insulin-resistant HepG2 cell model induction

Induction of the insulin resistance model (IRM) in HepG2 cells was done according to a previously reported protocol with slight modifications [23, 24]. Briefly, HepG2 cell seeding was done in 24-well plates at cell density of 6 $x10^3$ cells/well, in DMEM with high glucose concentration (25 mmol/L) for 24 h. Subsequently, media replacement with FBS-free high glucose DMEM containing insulin (10^{-7} mmol/L) was done, while leaving non-insulin-treated controls, followed by incubation for 24 h. IRM validation was performed by measuring the

ISSN: 3009-7061 **DOI: 10.21608/japs.2025.384682.1051**

glucose concentration in insulin and non-insulin-treated cells and subtracting it from blank culture media samples using glucose assay kit according to the instructions of the manufacturer at 546 nm.

2.4.4. Effect of K-NCDs on glucose uptake

To study K-NCDs effect on glucose uptake in HepG2/IRM and PANC-1 cells, cells were seeded at a density of 6 x10^3 cells/well for 24 h in a 24-well plate, then treated with K-NCDs in different concentrations (25-100 µg/mL). This was followed by measuring glucose concentration using the glucose assay kit in 10 µL of the medium.

2.4.5. *In vitro* anti-inflammatory effect

Following cells treatment with K-NCDs (50 µg/mL) and incubation for 24 h, HepG2/IRM and PANC-1 culture media were collected and centrifuged for 10 min at 200 g. Subsequently, the supernatant was analyzed using ELISA kits following the manufacturer's instructions for tumor necrosis factor alpha (TNF-α, Quantikine® ELISA # DTA00D) and interleukin-6 (IL-6, Quantikine® ELISA # D6050) levels.

2.5. *In vivo* oral hypoglycemic effect of K-NCDs

2.5.1. Animals

A week prior to the experiment, 18 male Wistar rats weighing 220 ± 20 g were obtained from the animal house (Faculty of Medicine, Alexandria University, Alexandria, Egypt) and allowed to acclimate. They were kept at room temperature and a regular 12-hour light/dark cycle. They also had unrestricted access to water and food. The Alexandria University Faculty of Pharmacy's Institutional Animal Care and Use Committee authorized the procedure (IRB No: 00012098, FWA NO: 00018699, Serial number: 0306629).

2.5.2. Induction of diabetes

For diabetes induction, the method reported by Dwivedi *et al*. was adopted with some modification [25]. Twelve rats were given a single dose of streptozotocin (STZ) equivalent to 40 mg/kg body weight, immediately dissolved in citrate buffer (0.1 M, pH 4.5) just before its intraperitoneal injection. To verify the onset of diabetes on the third day after the STZ injection, assessment of blood glucose level (BGL) using (Oncall plus®) glucose test strips was done. Diabetic rats were defined as those with postprandial blood glucose reading exceeding 250 mg/dL.

2.5.3. Oral glucose tolerance test (OGTT)

The hypoglycemic effect of K-NCDs, rats was studied. Rats were fasted overnight and then administered a single dose of glucose *via* intraperitoneal injection (2 g/kg). Rats were then assigned randomly to 2 groups. The positive control group: diabetic rats with no treatment, and K-NCDs treated group: diabetic rats were given 2 mL of K-NCDs as a single oral dose, equivalent to 400 mg/kg, one hour before the IP injection of glucose. A negative control group: healthy non-diabetic normal rats that didn't receive any treatments, was also included for comparison. Following glucose administration, BGL was measured at different time points (0-120 min).

2.6. Statistical analysis

Experimental findings are expressed as mean ± standard deviation (SD) of three independent tests at least. Statistical analysis was executed using GraphPad Prism (version 9.4.1, CA, USA) with statistical significance assessed using one-way analysis of variance (ANOVA) followed by Tukey's test for post hoc pair-wise comparisons. Results were considered statistically significant if $p \leq 0.05$.

3. Results and discussion

3.1. Preparation of K-NCDs, XRD, and FT-IR characterization

Kiwi derived nitrogen-doped carbon dots (K-NCDs) were synthesized using the solvothermal method, where kiwifruit juice and TEA acted as carbon and nitrogen sources, respectively. Kiwifruit was selected

ISSN: 3009-7061 **DOI: 10.21608/japs.2025.384682.1051**

as a carbon source as it is highly rich in ascorbic acid, which is its most distinctive nutritional peculiarity [26]. This is in addition to other bioactive molecules comprising carbon, nitrogen, and oxygen as their core elements [26, 27]. Upon solvothermal treatment for 3 h at 200°C, the solution turned brown and emitted greenish fluorescence under UV light.

The crystallinity of K-NCDs was investigated by XRD pattern (**Fig. 2a**). The spectrum revealed the typical wide-angle pattern previously reported for CDs [28]. The broad peak observed at $2\theta \approx 22.5°$ supports the amorphous nature of K-NCDs, which is coherent with the graphitic crystal lattice (002) plane of carbon-based materials [29, 30].

Surface functionalization of K-NCDs was identified from FT-IR spectrum (**Fig. 2b**). The spectrum exhibited a characteristic intense broad absorption band at 3366 cm^{-1}, corresponding to the O-H and N-H stretching vibrations. A weak absorption band at 2936.8 cm^{-1} assigned to the C-H stretching vibration is observed. An aromatic C=C signal at 1647.3 cm^{-1} previously ascribed to the sp^2-sp^3 hybridized honeycomb lattice of CD is also shown [28, 31]. Moreover, the peak at 1253.7 cm^{-1} indicates the presence of epoxy groups representative of typical graphitic carbon [31]. The low intensity of the CH_2 functional group and the high intensity of the C=C functional group reflect carbon dot formation *via* the solvothermal process. The spectrum obtained is consistent with previously reported FT-IR spectra of nitrogen-doped CDs [28, 30].

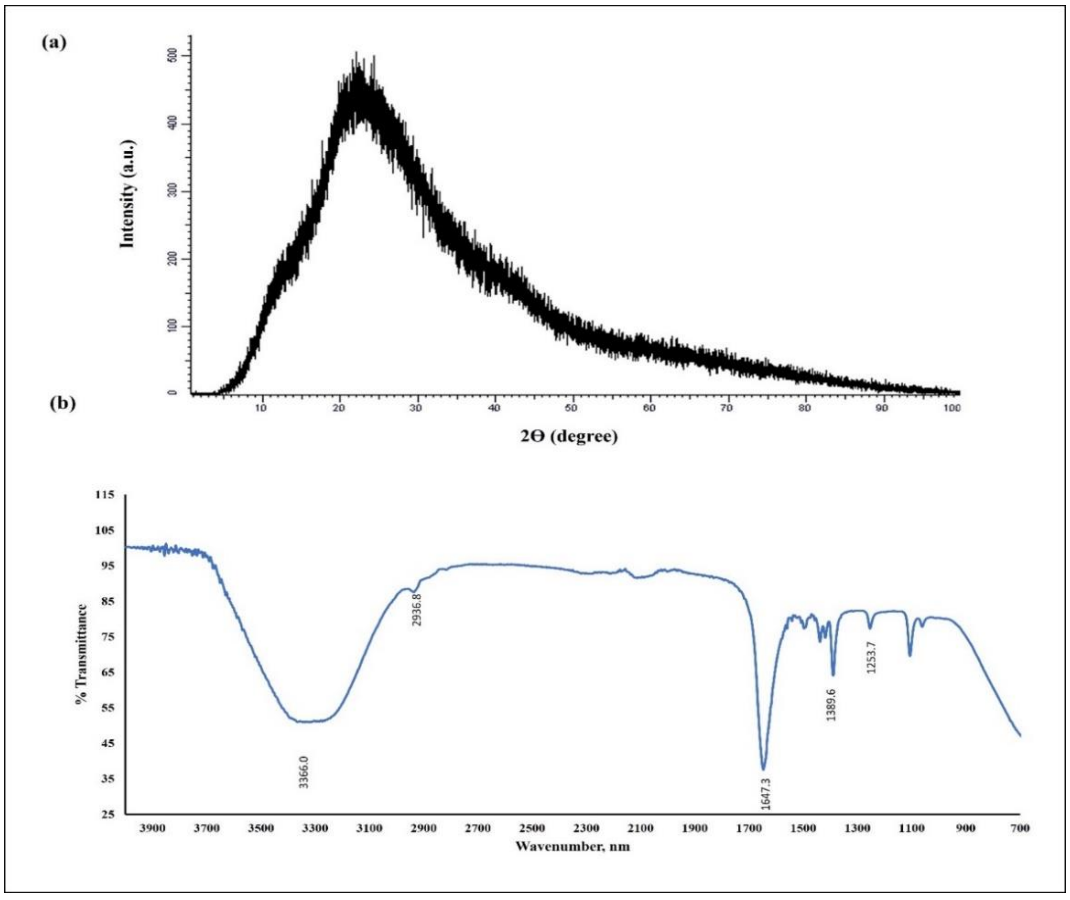

Fig. 2: (a) XRD pattern and (b) FT-IR spectrum of K-NCDs.

ISSN: 3009-7061 **DOI: 10.21608/japs.2025.384682.1051**

3.2. Morphological examination, particle size and zeta potential measurement

The morphological structure and size of K-NCDs were investigated by SEM and TEM imaging (**Fig. 3a & 3b**). Particles were shown to be quasi-spherical. Particle size assessment of K-NCDs based on the TEM images indicated a particle size in the range of 5–15 nm with an average size of 9.2 ± 3 nm. The size distribution histogram (**Fig. 3c**) reveals a narrow size distribution for K-NCDs. Also, K-NCDs showed a negative ζ-potential of -26.1±1.85 mV, indicating good colloidal stability.

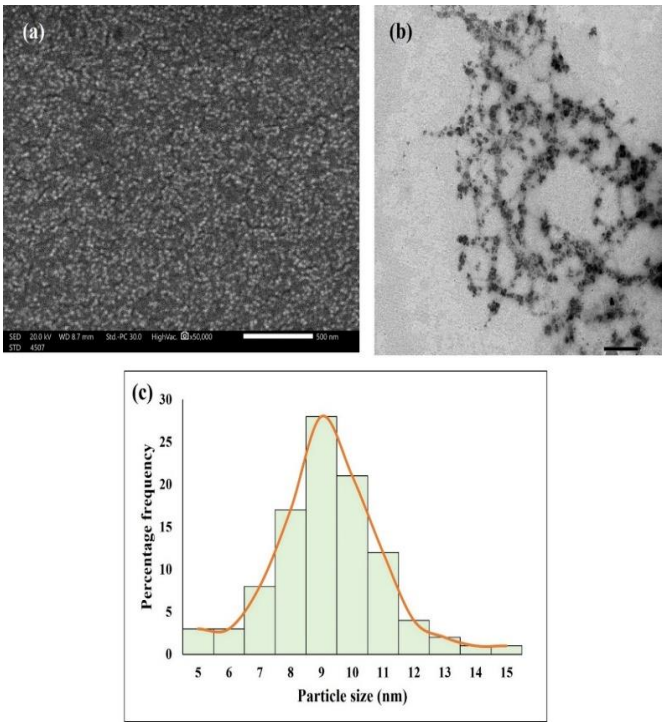

Fig. 3: (a) SEM image x50K, (b) TEM image x40K and (c) Particle size distribution curve of K-NCDs.

The negative zeta potential of KNCDs is primarily due to the presence of deprotonated oxygen-containing functional groups (especially carboxylic acids) on their surfaces. While ethylene diamine introduces nitrogen-containing groups, the overall effect often enhances or modifies the surface chemistry in a way that favors a net negative charge under neutral to basic conditions [32].

3.3. Optical properties

The optical properties of K-NCDs were studied using absorption and fluorescence spectra (**Fig. 4**). UV spectrum of K-NCDs displayed shoulders at 225 and 275 nm (**Fig. 4a**), which are ascribed to the π-π* transitions of carbon skeleton and conjugated sp^2 domains rich in π-electrons, and n- π* electronic transitions associated with heteroatoms, respectively. The fluorescence emission spectrum of K-NCDs at an excitation wavelength of 275 nm is shown in **Fig. 4b**. The inset shows the brown color of aqueous K-NCDs solution under visible light, whereas under UV light, green fluorescence is observed. The fluorescence results from excited defects of the surface states in nitrogen-doped CDs [41]. The fluorescence spectra of K-NCDs at different excitation wavelengths (**Fig. 4c**) demonstrated excitation-dependent emission behavior where the emission peak is red-shifted from 500 to 580 nm with an increment increase in excitation wavelength from 240 to 280 nm. The emission peak intensity increased initially with increasing excitation wavelength, with a maximum intensity reached at 275 nm excitation. This behavior has been previously attributed to K-NCDs particle size variation in addition to the distribution of various surface states resulting from different organic groups on K-NCDs surface [33].

The K-NCDs showed a high relative fluorescence QY of 37.9 % using FITC as a reference. The high QY observed could be attributed to the doping of the carbon framework with nitrogen [34].

ISSN: 3009-7061 **DOI: 10.21608/japs.2025.384682.1051**

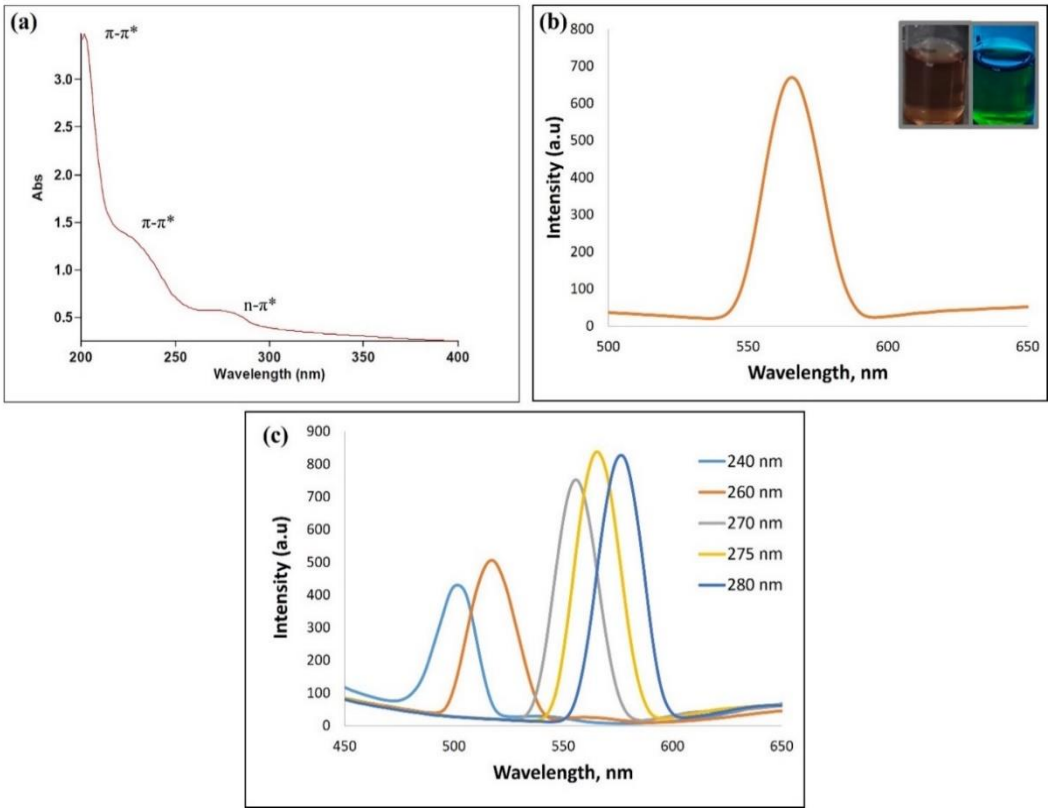

Fig. 4: (a) UV–Vis spectrum, (b) Fluorescence spectrum at 275 nm excitation wavelength (insets: images of K-NCDs under (left) visible light and (right) ultraviolet light) and (c) Emission spectra of K-NCDs at different excitation wavelengths (240-280 nm).

3.4. *In vitro* antioxidant effect of K-NCDs

Oxidative stress is considered a main factor in the development of the microvascular and cardiovascular complications of diabetes mellitus [35]. CDs have been found to possess antioxidative activity [36]. Kiwifruit itself has been reported to scavenge free radicals and reduce oxidative stress [37]. The antioxidant potential of K-NCDs was studied using DPPH radical scavenging activity (RSA) and catalase-like activity assays (**Fig. 5**). In order to test the ability of K-NCDs to scavenge free radicals, DPPH, a method based on the scavenging of the 2,2 diphenyl-1-picrylhydrazyl (DPPH) free radical was used [38]. DPPH RSA of increasing concentrations of K-NCDs (1.25-5 mg/mL) is shown in **Fig. 5a**. A significant increase in antioxidant activity ($p \leq 0.05$) was observed with increasing concentration to reach 99.6 % for the 5 mg/mL sample, reflecting the radical scavenging potential of K-NCDs. This concentration-dependent RSA of K-NCDs has been previously reported for other CDs prepared from natural products [39, 40]. A possible explanation is through the transfer of hydrogen from CDs surface groups (carboxyl, hydroxyl, and amino groups) to DPPH and hence its reduction to DPPH-H [41]. This is in addition to the sp^2-rich domains which favor adducts formation with radical species [41].

The catalase-like action of K-NCDs was studied by assessing their H_2O_2 scavenging effect. Catalase is a strong natural antioxidant proven to be cardinal in cell protection against oxidative damage *via* catalyzing H_2O_2 degradation [42]. As shown in **Fig. 5b**, catalase-like activity increased significantly in a dose-dependent manner ($p \leq 0.05$). This

ISSN: 3009-7061 **DOI: 10.21608/japs.2025.384682.1051**

H_2O_2 scavenging effect mimicking catalase activity has been previously reported for CDs and was ascribed to their distinct surface chemistry and functional groups, which promote the catalytic decomposition of H_2O_2 [43]. Besides oxidative stress reduction, H_2O_2 scavenging was shown to upregulate the activity of the antioxidant enzyme (NQO1) in endothelial cells, thereby inhibiting TNF-α-induced endothelial inflammation [43]. Also, Muhammad *et al*. relayed the success of CDs as single-atom nanozyme-mediated catalytic therapy for glioblastoma, referring to the potential of nitrogen doping to enhance catalase-like activity [44].

3.5. *In vitro* yeast glucose uptake assay

The effect of different concentrations of K-NCDs (0.5-5 mg/mL) on glucose uptake by yeast cells was tested (**Fig. 5c**). The results revealed a significant increase in the % of glucose uptake with increasing concentration with 5 mg concentration achieving 92.05 ± 2.25% increase in glucose uptake vs 16.81 ±2.19, 23.38 ± 2.02 and 47 ± 4.1% for 0.5, 1.25 and 2.5 mg/mL, respectively ($p \leq 0.001$). Yeast cells exhibit a different glucose uptake mechanism compared to animal cells, as yeast utilizes mainly facilitated diffusion, with glucose uptake being affected by several factors such as the internal glucose concentration and the rate of sugar conversion into various metabolites [45]. Despite this mechanistic distinction, the results of glucose uptake by yeast cells were formerly shown to reflect the effect of different treatments on the enhanced glucose uptake by muscle cells and adipose tissues [46, 47]. Parvathy *et al*. previously reported the hypoglycemic potential of grape seed-derived carbon dots and their ability to effectively bind glucose due to facilitated diffusion and enhanced glucose metabolism through the yeast cell membrane [47].

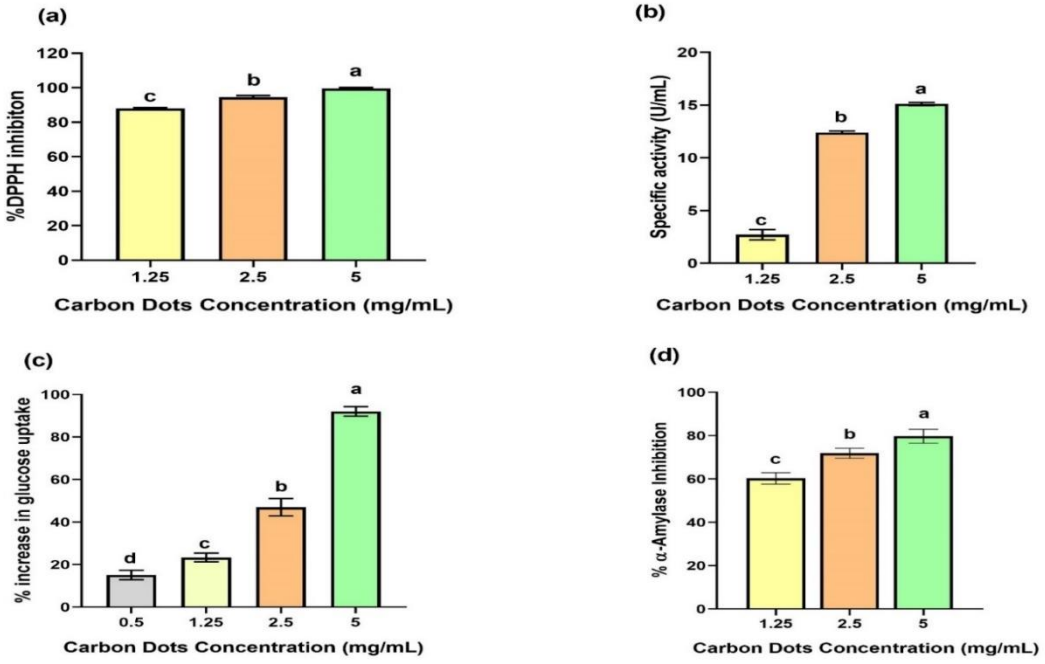

Fig. 5: (a) Percentage DPPH inhibition, (b) Catalase-like activity (U/mL), (c) Percentage increase in glucose uptake by yeast cells, and (d) Percentage α-amylase inhibition of increasing K-NCDs amounts. Results were presented as mean±SD (n=3) and analyzed using one-way ANOVA followed by Tukey's post-hoc test for group comparisons. Means of similar symbols were statistically insignificant: a>b>c>d ($p \leq 0.05$).

ISSN: 3009-7061 **DOI: 10.21608/japs.2025.384682.1051**

3.6. *In vitro* α-amylase inhibition

Amylase is an enzyme that helps digest starch by converting it into monosaccharides, which can result in elevated blood sugar levels [48]. As a result, inhibiting α-amylase is considered a potential target for managing type 2 diabetes [49]. It has been shown that kiwifruit slows starch digestion through α-amylase inactivation, thus reducing the blood sugar level [50]. In the current study, the antidiabetic potential of K-NCDs was assessed by estimating the amylase-inhibitory action. Increasing concentrations (1.25-5 mg/mL) of K-NCDs were used. A dose-dependent inhibition was observed (**Fig. 5d**) with 5 mg/mL K-NCDs showing the greatest α-amylase inhibitory effect (79.7 ± 2.66%) ($p \leq 0.001$). Similar α-amylase suppression activity was reported for carbon dots doped with heteroatoms (fluorine and nitrogen) and prepared using the solvothermal technique from either powdered leaves of various medicinal plants or zaltoprofen (an anti-inflammatory drug) in the presence of 4,5-difluoro-1,2-benzenediamine (DFBD) as a fluorine and nitrogen source [51]. Additionally, the α-amylase inhibitory potential of *Acetosa Sagittata*-derived CDs was ascribed to the presence of surface functional groups (amino, carboxyl, and hydroxyl) that could interact with enzyme active sites through hydrogen or covalent bonding as well as electrostatic interactions. Another possible explanation was that CDs can chelate metal ions, which are necessary as cofactors for enzymes [52].

3.7. Cell culture studies

3.7.1. Cytotoxicity assay

The MTT assay was used to examine the cytotoxicity of different concentrations of K-NCDs (2-100 µg/mL) on HepG2 and PANC-1 cells. In the concentration range studied, none of the tested samples exhibited any cytotoxicity towards cells with % cell viability > 90%, reflecting biocompatibility and safety (**Fig. 6a & b**). The biocompatibility of CDs is well documented [53]. Magalhães *et al*. reported that N-doped CDs have no discernible effect on the cell viability of the tested cancer cells (A549 and UM-UC-5), suggesting their suitability for bioimaging applications [54]. Also, CDs prepared from banana biomass showed no noxious effects on HDF cell viability [55].

3.7.2. Evaluation of glucose uptake

In this test, the insulin-sensitizing power of the prepared K-NCDs on two insulin-resistant (IR) cell line models (HepG2/IRM & PANC-1) was explored. Whereas IRM was induced in HepG2 cells [23], the previously reported ability of pancreatic cancer cell line supernatants to induce β-cell dysfunction both *in vitro* and *in vivo*, as well as insulin resistance in cultured myoblasts and hepatocytes [56], reflects the innate insulin resistance of PANC-1.

As seen in **Fig. 6c & d**, treatment of either HepG2/IRM or PANC-1 cells with increasing concentrations of K-NCDs (25-100 µg/mL) resulted in a significant ($p \leq 0.05$) increase in glucose uptake in a dose-dependent manner in comparison to control, untreated cells, verifying the insulin-sensitizing potential of K-NCDs. This might be ascribed to the ability of K-NCDs to inhibit both inflammation and oxidative stress as contributors to insulin resistance. The results obtained are supported by the *in vitro* antioxidant potential of K-NCDs as shown by the DPPH RSA and catalase-like effects. Indeed, the anti-inflammatory power of CDs mediated *via* decreasing the levels of pro-inflammatory cytokines (TNF-α & IL-6) has been documented [57]. Also, CDs were reported to reduce oxidative stress by markedly raising the levels of antioxidant enzymes [58].

ISSN: 3009-7061 **DOI: 10.21608/japs.2025.384682.1051**

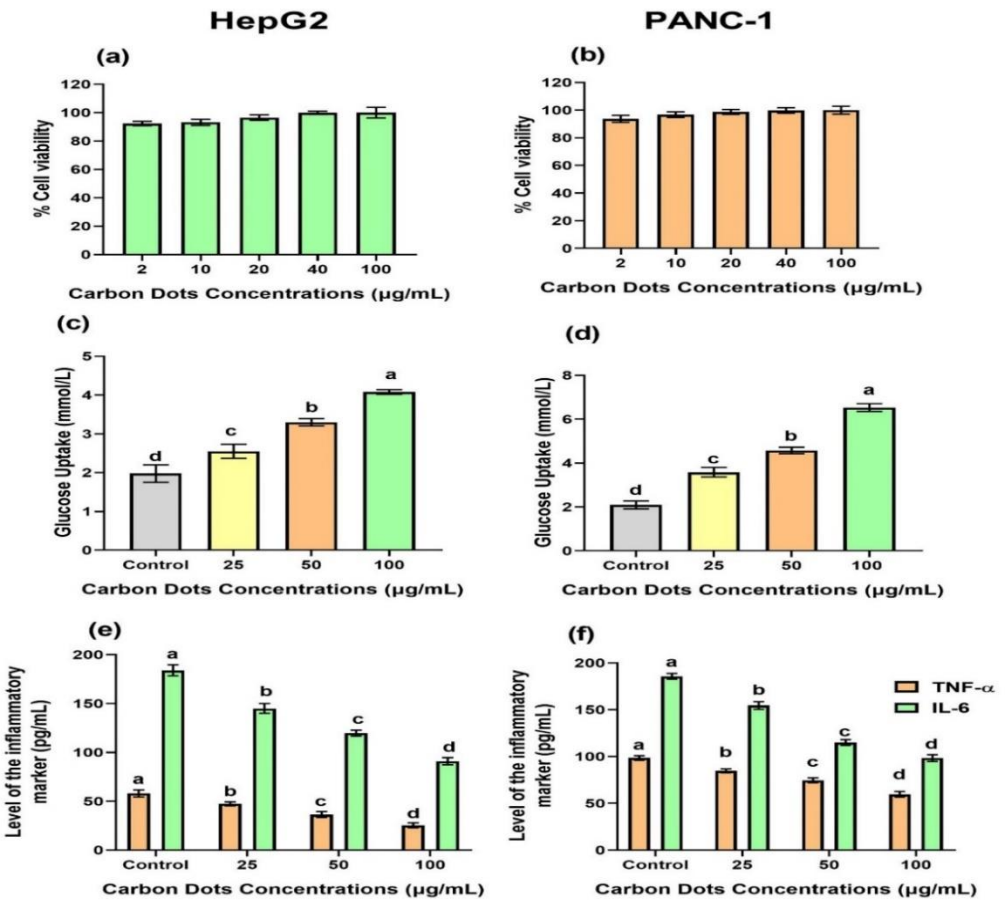

Fig. 6:(a, b) Percentage cell viability of HepG2 and PANC-1 treated with increasing concentrations of K-NCDs (2-100 µg/mL) for 48 h. (c, d) Effect of increasing concentrations of carbon dots (25-100 µg/mL) on glucose uptake by HepG2/IRM and PANC-1 cells after K-NCDs treatment. (e, f) Effect of K-NCDs on the inflammatory markers, TNF-α and IL-6 for HepG2/IRM and PANC-1 cells. Results were presented as mean±SD (n=3) and analyzed using one-way anova followed by Tukey's post-hoc test for group comparisons. Means of similar symbols were statistically insignificant: a>b>c>d ($p \leq 0.05$).

3.7.3. *In vitro* assessment of anti-inflammatory effect

Since genes for many proinflammatory cytokines, such as TNF-α & IL-6, are overexpressed in cells as insulin resistance develops [23], the levels of these markers were investigated after treatment of the tested IR-cells (HepG2/IRM and PANC-1) with the K-NCDs (25-100 µg/mL). As demonstrated in **Fig. 6e&f**, the control IR-cells presented a significant elevation in the inflammatory markers compared to those treated with K-NCDs ($p \leq 0.05$), further proving inflammation as one of the well-reported mechanisms for insulin resistance. On the other hand, treatment with increasing concentration of K-NCDs resulted in a significant reduction ($p \leq 0.05$) in both TNF-α and IL-6 vs the control cells in a dose-dependent manner, confirming their anti-inflammatory potential and elucidating their mechanism of action in reversing insulin resistance. The *in vitro* anti-inflammatory properties of CDs were confirmed by Dong *et al*. where CDs nanozyme achieved a significant reduction in TNF-α and IL-6 in

ISSN: 3009-7061 **DOI: 10.21608/japs.2025.384682.1051**

lipopolysaccharide-induced RAW264.7 cells inflammation model [59]. This could be ascribed to the ROS scavenging ability of CDs nanozyme conferred by their superior electron donor and electron acceptor capabilities [59]. Additionally, CDs were reported to suppress LPS-induced liver inflammation in mice after their IV administration in a dose-dependent manner owing to the proven ability to reduce the elevated ROS levels caused by LPS [60].

3.8. *In vivo* hypoglycemic effect

The hypoglycemic activity of CDs in diabetic rats has been previously reported *via* α-glucosidase inhibitory effect [61]. The α-glucosidase enzyme represents a therapeutic target to prevent postprandial hyperglycemia *via* retarding the carbohydrates absorption from the GIT [61]. Also, citric acid CDs showed rapid and effective glycolysis and hence lowered blood glucose levels by increasing metabolic activity after oral administration [62]. The oral hypoglycemic effect of the developed eco-friendly K-NCDs is shown in **Fig. 7**. All rats displayed low BGL at zero time owing to overnight fasting. Following IP glucose administration, the positive control group demonstrated a highly significant elevation in BGL vs the negative control one ($p \leq 0.0001$). On the other hand, treatment with K-NCDs prevented BGL shooting and achieved a significant reduction in BGL throughout the study period ($p \leq 0.0001$). Similarly, Zhao *et al*. reported the BGL-lowering effect of Zingiberis Carbonisata-based CDs [63]. The results observed could partly be explained by the demonstrated α-amylase inhibitory action of K-NCDs. Moreover, the anti-inflammatory and antioxidant effects observed for K-NCDs could have assisted in BGL control and OGT, as previous studies suggested improved insulin sensitivity and BGL control with reduced inflammation and oxidative damage [64]. Therefore, this study lays the foundation for further *in vivo* investigations to validate and elucidate the antihyperglycemic potential of K-NCDs in subsequent research.

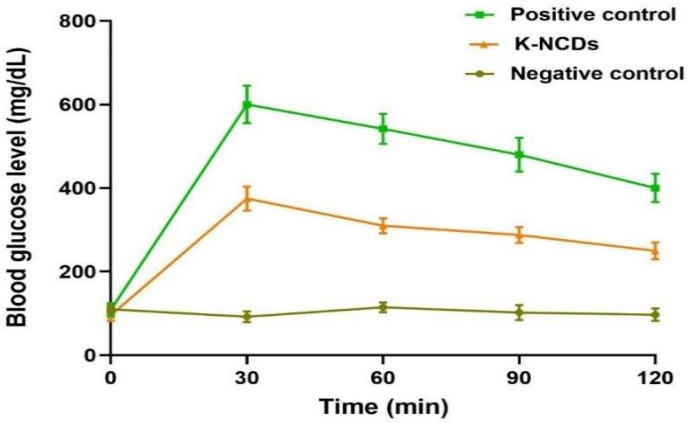

Fig. 7: Effect of K-NCDs on oral glucose tolerance. Data are expressed as mean±SD (n=6).

4. Conclusions

In the current work, nitrogen-doped carbon dots as a biocompatible nanomaterial were synthesized from Kiwifruit juice (K-NCDs). They were prepared by a single-step solvothermal process from kiwifruit juice and triethanolamine as the carbon and nitrogen precursors, respectively. The simple green low-cost method of preparation suggests the possibility for prospective synthesis on an industrial scale. The structure and surface functionalization of K-NCDs were revealed by XRD, FTIR, and microscope imaging. Structural characterization revealed CDs graphitic structure with successful nitrogen doping. The high quantum yield observed (37.9%) reflects K-NCDs high luminescent properties, suggesting their potential for future use in numerous bioimaging and biosensing applications. Here, the aptitude of K-NCDs as oral hypoglycemics was tested both *in vitro* and *in vivo*. The results showed that K-NCDs possess dose-dependent α-amylase inhibition, antioxidant, and anti-inflammatory effects. Also, their ability to increase glucose uptake by insulin-resistant cell lines reflects their capacity for insulin sensitization. Finally, K-NCDs prevented

ISSN: 3009-7061 **DOI: 10.21608/japs.2025.384682.1051**

BSL shooting in fasted diabetic mice following glucose administration. The results reflect the propensity of K-NCDs as a biocompatible oral treatment for hyperglycemia with immense potential for other biomedical applications. Future research should focus on detailed mechanistic studies and clinical trials to further validate the therapeutic potential of these green-synthesized CDs in managing diabetes.

Declaration of Competing Interest

The authors declare that they have no known competing financial interests or personal relationships that could have appeared to influence the work reported in this paper.

Data availability

Data will be made available on request

Funding

The authors declare that no fund was received from any organization for the submitted work.

Authors' contributions:

R.M.E Conceptualization; Methodology; Data curation; Formal analysis; Writing original draft; Writing - review & editing. **A.H.E** Conceptualization; Methodology; Resources; Writing - original draft; Writing - review & editing. **M.O.S** Data curation; Formal analysis; Methodology; Resources. **A.A.A** Methodology; Data curation; Formal analysis; Writing - original draft; Writing - review & editing

Highlights

- Sustainable and eco-friendly N-doped carbon dots were prepared from kiwifruit
- K-NCDs showed a high relative fluorescence quantum yield of 37.9 %
- Dose-dependent antioxidant, α-amylase inhibition, and catalase-like effects detected
- K-NCDs showed insulin resistance reversal *in vitro* in HepG2/IRM and PANC-1 cells
- Oral hypoglycemic efficacy following K-NCDs oral administration in diabetic rat model

5. References

(1) International Diabetes Federation. International Diabetes Federation Diabetes Atlas. 2023. Available from: https://diabetesatlas.org/.

(2) Heller SR, Geybels MS, Iqbal A, Liu L, Wagner L, Chow E. A higher non-severe hypoglycaemia rate is associated with an increased risk of subsequent severe hypoglycaemia and major adverse cardiovascular events in individuals with type 2 diabetes in the LEADER study. Diabetologia. 2022;65:55-64.

(3) Bhatia S. Nanoparticles types, classification, characterization, fabrication methods and drug delivery applications. Natural polymer drug delivery systems: Nanoparticles, plants, and algae. 2016:33-93.

(4) Cui L, Ren X, Sun M, Liu H, Xia L. Carbon dots: Synthesis, properties and applications. Nanomaterials. 2021;11(12):3419.

(5) Sahana S, Gautam A, Singh R, Chandel S. A recent update on development, synthesis methods, properties and application of natural products derived carbon dots. Natural Products and Bioprospecting. 2023;13(1):51.

(6) Yao L, Zhao M-M, Luo Q-W, Zhang Y-C, Liu T-T, Yang Z, et al. Carbon quantum dots-based nanozyme from coffee induces cancer cell ferroptosis to activate antitumor immunity. ACS nano. 2022;16(6):9228-39.

(7) Qureshi WA, Vivekanandan B, Jayaprasath JA, Ali D, Alarifi S, Deshmukh K. Antimicrobial Activity and Characterization of Pomegranate Peel-Based Carbon Dots. Journal of Nanomaterials. 2021;2021(1):9096838.

(8) Prakash A, Muthu M, Raja G, Gopal J. Preparation and Characterization of Carbon Nanodots from turmeric soot for anti-coliform and anti-oral bacterial applications and as anti-staphylococcal coatings. Nanotheranostics. 2025;9(1):31.

(9) Humaera NA, Fahri AN, Armynah B, Tahir D. Natural source of carbon dots from part of a plant and its applications: a review. Luminescence. 2021;36(6):1354-64.

(10) Zeng M, Wang Y, Liu M, Wei Y, Wen J, Zhang Y, et al. Potential efficacy of herbal medicine-derived Carbon Dots in the treatment of diseases: from mechanism to clinic. International Journal of Nanomedicine. 2023:6503-25.

(11) Guo S, Zhang R, Liu Y, Zhang Q, Liu X, Wu X, et al. Synthesis, applications in therapeutics, and bioimaging of traditional Chinese medicine-derived carbon dots. Carbon Letters. 2024;34(2):545-64.

(12) Lu F, Zhang Y, Cheng J, Zhang M, Luo J, Qu H, et al. Maltase and sucrase inhibitory activities and hypoglycemic effects of carbon dots derived from charred Fructus crataegi. Materials Research Express. 2019;6(12):125005.

(13) Sun Z, Lu F, Cheng J, Zhang M, Zhu Y, Zhang Y, et al. Hypoglycemic bioactivity of novel eco-friendly carbon dots derived from traditional Chinese medicine. Journal of Biomedical

ISSN: 3009-7061 **DOI: 10.21608/japs.2025.384682.1051**

Nanotechnology. 2018;14(12):2146-55.
(14) El Azab EF, Alakilli SYM, Saleh AM, Alhassan HH, Alanazi HH, Ghanem HB, et al. Actinidia deliciosa Extract as a Promising Supplemental Agent for Hepatic and Renal Complication-Associated Type 2 Diabetes (In Vivo and In Silico-Based Studies). Int J Mol Sci. 2023;24(18).
(15) Satpal D, Kaur J, Bhadariya V, Sharma K. Actinidia deliciosa (Kiwi fruit): A comprehensive review on the nutritional composition, health benefits, traditional utilization, and commercialization. Journal of Food processing and Preservation. 2021;45(6):e15588.
(16) Mechchate H, Es-Safi I, Haddad H, Bekkari H, Grafov A, Bousta D. Combination of Catechin, Epicatechin, and Rutin: Optimization of a novel complete antidiabetic formulation using a mixture design approach. The Journal of Nutritional Biochemistry. 2021;88:108520.
(17) Arul V, Sethuraman MG. Facile green synthesis of fluorescent N-doped carbon dots from Actinidia deliciosa and their catalytic activity and cytotoxicity applications. Optical Materials. 2018;78:181-90.
(18) Atchudan R, Kishore SC, Gangadaran P, Edison TNJI, Perumal S, Rajendran RL, et al. Tunable fluorescent carbon dots from biowaste as fluorescence ink and imaging human normal and cancer cells. Environmental Research. 2022;204:112365.
(19) Wang K, Li M, Han Q, Fu R, Ni Y. Inhibition of α-amylase activity by insoluble and soluble dietary fibers from kiwifruit (Actinidia deliciosa). Food Bioscience. 2021;42:101057.
(20) Aboul-Enein A, Salama DZ, Gaafar A, Aly H, Ahmed H. Comparative hypoglycemic effect of acetone extract of banana (Musa paradisiaca), kiwi (Actinidia deliciosa planch) and olive (Olea europaea L.), byproducts. Bioscience Research. 2019;16:854-69.
(21) Rehman G, Hamayun M, Iqbal A, Ul Islam S, Arshad S, Zaman K, et al. In Vitro Antidiabetic Effects and Antioxidant Potential of Cassia nemophila Pods. Biomed Res Int. 2018;2018:1824790.
(22) Wickramaratne MN, Punchihewa JC, Wickramaratne DB. In-vitro alpha amylase inhibitory activity of the leaf extracts of Adenanthera pavonina. BMC Complement Altern Med. 2016;16(1):466.
(23) Soliman MO, El-Kamel AH, Shehat MG, Bakr BA, El-Moslemany RM. Lactoferrin decorated bilosomes for the oral delivery of quercetin in type 2 diabetes: In vitro and in vivo appraisal. Int J Pharm. 2023;647:123551.
(24) Gao F, Jian L, Zafar MI, Du W, Cai Q, Shafqat RA, et al. 4-Hydroxyisoleucine improves insulin resistance in HepG2 cells by decreasing TNF-α and regulating the expression of insulin signal transduction proteins. Mol Med Rep. 2015;12(5):6555-60.
(25) Dwivedi S, Gottipati A, Ganugula R, Arora M, Friend R, Osburne R, et al. Oral Nanocurcumin Alone or in Combination with Insulin Alleviates STZ-Induced Diabetic Neuropathy in Rats. Mol Pharm. 2022;19(12):4612-24.
(26) Richardson DP, Ansell J, Drummond LN. The nutritional and health attributes of kiwifruit: a review. Eur J Nutr. 2018;57(8):2659-76.
(27) Yu M, Man Y, Lei R, Lu X, Wang Y. Metabolomics Study of Flavonoids and Anthocyanin-Related Gene Analysis in Kiwifruit (Actinidia chinensis) and Kiwiberry (Actinidia arguta). Plant Molecular Biology Reporter. 2020;38(3):353-69.
(28) Atchudan R, Edison TNJI, Lee YR. Nitrogen-doped carbon dots originating from unripe peach for fluorescent bioimaging and electrocatalytic oxygen reduction reaction. Journal of Colloid and Interface Science. 2016;482:8-18.
(29) Prathap N, Balla P, Shivakumar MS, Periyasami G, Karuppiah P, Ramasamy K, et al. Prosopis juliflora hydrothermal synthesis of high fluorescent carbon dots and its antibacterial and bioimaging applications. Scientific Reports. 2023;13(1):9676.
(30) Kundu A, Maity B, Basu S. Orange Pomace-Derived Fluorescent Carbon Quantum Dots: Detection of Dual Analytes in the Nanomolar Range. ACS Omega. 2023;8(24):22178-89.
(31) Georgakilas V, Perman JA, Tucek J, Zboril R. Broad Family of Carbon Nanoallotropes: Classification, Chemistry, and Applications of Fullerenes, Carbon Dots, Nanotubes, Graphene, Nanodiamonds, and Combined Superstructures. Chemical Reviews. 2015;115(11):4744-822.
(32) Afshary H, Amiri M, Bezaatpour A, Wark M. Electrochemiluminescence sensor based on N-doped carbon quantum dots for determination of ceftazidime in real samples. J Electrochem Soc. 2022;169(2):026523.
(33) John BK, John N, Korah BK, Thara C, Abraham T, Mathew B. Nitrogen-doped carbon quantum dots as a highly selective fluorescent and electrochemical sensor for tetracycline. Journal of Photochemistry and Photobiology A: Chemistry. 2022;432:114060.
(34) Manioudakis J, Victoria F, Thompson CA, Brown L, Movsum M, Lucifero R, et al. Effects of nitrogen-doping on the photophysical

ISSN: 3009-7061 **DOI: 10.21608/japs.2025.384682.1051**

properties of carbon dots. Journal of Materials Chemistry C. 2019;7(4):853-62.
(35) Bhatti JS, Sehrawat A, Mishra J, Sidhu IS, Navik U, Khullar N, et al. Oxidative stress in the pathophysiology of type 2 diabetes and related complications: Current therapeutics strategies and future perspectives. Free Radical Biology and Medicine. 2022;184:114-34.
(36) Dong C, Wang S, Ma M, Wei P, Chen Y, Wu A, et al. Inhibition of oxidative stress in vivo through enzyme-like activity of carbon dots. Applied Materials Today. 2021;25:101178.
(37) Wang Y, Li L, Liu H, Zhao T, Meng CW, Liu Z, et al. Bioactive compounds and in vitro antioxidant activities of peel, flesh and seed powder of kiwi fruit. International Journal of Food Science & Technology. 2018;53:2239–45.
(38) Baliyan S, Mukherjee R, Priyadarshini A, Vibhuti A, Gupta A, Pandey RP, et al. Determination of Antioxidants by DPPH Radical Scavenging Activity and Quantitative Phytochemical Analysis of Ficus religiosa. Molecules. 2022;27(4):1326.
(39) Murru C, Badía-Laíño R, Díaz-García ME. Synthesis and Characterization of Green Carbon Dots for Scavenging Radical Oxygen Species in Aqueous and Oil Samples. Antioxidants. 2020;9(11):1147.
(40) Yang D, Li L, Cao L, Chang Z, Mei Q, Yan R, et al. Green Synthesis of Lutein-Based Carbon Dots Applied for Free-Radical Scavenging within Cells. Materials. 2020;13(18):4146.
(41) Innocenzi P, Stagi L. Carbon dots as oxidant-antioxidant nanomaterials, understanding the structure-properties relationship. A critical review. Nano Today. 2023;50:101837.
(42) Leonida MD, Kumar I, Elshaer MR, Mahmoud Z, Lozanovska B, Bijja UK, et al. Ecofriendly approaches to efficiently enhance catalase performance. International Journal of Biological Macromolecules. 2024;280:135597.
(43) Chavez J, Khan A, Watson KR, Khan S, Si Y, Deng AY, et al. Carbon Nanodots Inhibit Tumor Necrosis Factor-α-Induced Endothelial Inflammation through Scavenging Hydrogen Peroxide and Upregulating Antioxidant Gene Expression in EA.hy926 Endothelial Cells. Antioxidants. 2024;13(2):224.
(44) Muhammad P, Hanif S, Li J, Guller A, Rehman FU, Ismail M, et al. Carbon dots supported single Fe atom nanozyme for drug-resistant glioblastoma therapy by activating autophagy-lysosome pathway. Nano Today. 2022;45:101530.
(45) Rehman G, Hamayun M, Iqbal A, Islam S, Arshad S, Zaman K, et al. In Vitro Antidiabetic Effects and Antioxidant Potential of Cassia nemophila Pods. BioMed Research International. 2018;2018:6.
(46) Harish M, Ahmed F, Urooj A. In vitro hypoglycemic effects of Butea monosperma Lam. leaves and bark. J Food Sci Technol. 2014;51(2):308-14.
(47) Parvathy C, P.K P. Evaluation of Anti-diabetic Potential of Anti-microbial Carbon Quantum Dots from Vitis Vinifera Seeds. Nano Biomedicine and Engineering. 2023;15.
(48) Kaur N, Kumar V, Nayak SK, Wadhwa P, Kaur P, Sahu SK. Alpha-amylase as molecular target for treatment of diabetes mellitus: A comprehensive review. Chemical Biology & Drug Design. 2021;98(4):539-60.
(49) Gong L, Feng D, Wang T, Ren Y, Liu Y, Wang J. Inhibitors of α-amylase and α-glucosidase: Potential linkage for whole cereal foods on prevention of hyperglycemia. Food Science & Nutrition. 2020;8(12):6320-37.
(50) Dhiman VK, Chauhan V, Kanwar SS, Singh D, Pandey H. Purification and characterization of actinidin from Actinidia deliciosa and its utilization in inactivation of α-amylase. Bulletin of the National Research Centre. 2021;45(1):213.
(51) Kota S, Dumpala P, Sajja R, Anantha R. Heteroatom-doped carbon dots from medicinal plants as novel biomaterials for as-use biomedical applications in comparison with synthetic drug, zaltoprofen. Scientific Reports. 2024;14(1):13160.
(52) Prasada P, Nirmalab PV. Green Carbon Dots Derived From Acetosa Sagittata Aerial Parts And In Vitro Antidiabetic, Antioxidant And Cytotoxic Properties. Revista Argentina de Clínica Psicológica 2023;XXXII:63-71
(53) Park Y, Kim Y, Chang H, Won S, Kim H, Kwon W. Biocompatible nitrogen-doped carbon dots: synthesis, characterization, and application. Journal of Materials Chemistry B. 2020;8(39):8935-51.
(54) Magalhaes CM, Ribeiro E, Fernandes S, Esteves da Silva J, Vale N, Pinto da Silva L. Safety Evaluation of Carbon Dots in UM-UC-5 and A549 Cells for Biomedical Applications. Cancers (Basel). 2024;16(19).
(55) Patel DK, Won S-Y, Jung E, Deb Dutta S, Patil TV, Lim K-T, et al. Assessment of the biocompatibility and bioimaging potential of fluorescent carbon dots derived from waste biomass. Materials Letters. 2024;361:136152.
(56) Salvatore T, Marfella R, Rizzo MR, Sasso FC. Pancreatic cancer and diabetes: A two-way relationship in the perspective of diabetologist.

ISSN: 3009-7061 **DOI: 10.21608/japs.2025.384682.1051**

Int J Surg. 2015;21 Suppl 1:S72-7.
(57) Kumar M, Chinnathambi S, Bakhori N, Abu N, Etezadi F, Thangavel V, et al. Biomass-derived carbon dots as fluorescent quantum probes to visualize and modulate inflammation. Sci Rep. 2024;14(1):12665.
(58) Sharma A, Choi HK, Lee HJ. Carbon Dots for the Treatment of Inflammatory Diseases: An Appraisal of In Vitro and In Vivo Studies. Oxid Med Cell Longev. 2023;2023:3076119.
(59) Dong C, Ma X, Huang Y, Zhang Y, Gao X. Carbon dots nanozyme for anti-inflammatory therapy via scavenging intracellular reactive oxygen species. Front Bioeng Biotechnol. 2022;10:943399.
(60) Kong B, Yang T, Cheng F, Qian Y, Li C, Zhan L, et al. Carbon dots as nanocatalytic medicine for anti-inflammation therapy. J Colloid Interface Sci. 2022;611:545-53.
(61) Shao T, Yuan P, Zhu L, Xu H, Li X, He S, et al. Carbon Nanoparticles Inhibit ?-Glucosidase Activity and Induce a Hypoglycemic Effect in Diabetic Mice. Molecules. 2019;24(18):3257.
(62) Camlik G, Ozakca I, Bilakaya B, Ozcelikay AT, Velaro AJ, Wasnik S, et al. Development of composite carbon quantum dots-insulin formulation for oral administration. Journal of Drug Delivery Science and Technology. 2022;76:103833.
(63) Zhao J, Zhang Y, Zhao Y, Wu T, Chen Y, Zhang Y, et al. Protective Effects of Zingiberis Carbonisata-Based Carbon Dots on Diabetic Liver Injury in Mice. Journal of Biomedical Nanotechnology. 2022;18(8):1975-85.
(64) Rochette L, Zeller M, Cottin Y, Vergely C. Diabetes, oxidative stress and therapeutic strategies. Biochim Biophys Acta, Gen Subj. 2014;1840(9):2709-29.

ISSN: 3009-7061 **DOI: 10.21608/japs.2025.384682.1051**